Application of neural networks to digital pulse shape analysis for an array of silicon strip detectors

J. L. Flores[a], I. Martel[b,d], R. Jiménez[c], J. Galán[c,*] and P. Salmerón[a]

[a]Dpto de Ingeniería Eléctrica y Térmica, Universidad de Huelva, Spain
[b]Dpto de Física Aplicada, Universidad de Huelva
[c]Dpto de Ingeniería Electrónica, Sist. Informáticos y Automática, Universidad de Huelva
[d]CERN, ISOLDE, CH 1211 Geneva, 23, Switzerland

Abstract

The new generation of nuclear physics detectors that used to study nuclear reactions is considering the use of digital pulse shape analysis techniques (DPSA) to obtain the (A,Z) values of the reaction products impinging in solid state detectors. This technique can be an important tool for selecting the relevant reaction channels at the HYDE (HYbrid DEtector ball array) silicon array foreseen for the Low Energy Branch of the FAIR facility (Darmstadt, Germany). In this work we study the feasibility of using artificial neural networks (ANNs) for particle identification with silicon detectors. Multilayer Perceptron networks were trained and tested with recent experimental data, showing excellent identification capabilities with signals of several isotopes ranging from ^{12}C up to ^{84}Kr, yielding higher discrimination rates than any other previously reported.

Keywords: HYDE, FAIR, Neural Networks, Digital Pulse Shape Analysis, Silicon Detectors.

1. Introduction

The nuclei near the drip lines are very different from stable nuclei, and radioactive beam facilities (RBF) provide a unique workbench to investigate nuclear structure and dynamics by exploiting the isospin degree of freedom. There is a number of new RBF foreseen to be operative in the next two decades, like SPIRAL2 at GANIL [1], FAIR at GSI [2], SPES at LNL [3] and EURISOL [4], which will accelerate radioactive nuclear beams (RNB) with intensities several orders of magnitude higher than today's ones, allowing the study of very rare and short-lived nuclei not presently available. This will demand very powerful detection

* Corresponding author.
E-mail address: jgalan@diesia.uhu.es (J. Galán)

systems capable of fully identifying the reaction products over the largest dynamical range and with the lowest possible thresholds.

One of these instruments, the HYDE silicon array (HYbrid DEtector ball array), is foreseen for carrying nuclear spectroscopy Studies at the Low Energy Branch of the new accelerator facility FAIR being built at GSI (Darmstadt, Germany) [2]. The purpose of this device is the study of nuclear reactions induced by exotic isotopes in a range of collision energies below 30 A MeV. In its present design the proposed detector array should contain 50 detector cells made of five layers of multi-strip silicon detectors for charged particle detection. To carry out the physics program an efficient particle-identification tool is needed for reaction channel selection and data analysis.

Particle identification (PID) is normally achieved by time of flight (TOF) and energy loss (ELOSS) techniques. The former requires long flight paths which translate into large, expensive and somewhat cumbersome arrays. The latter implies relatively high thresholds which preclude the identification of both low energy and very fast particles. A third technique for PID is based on analog pulse shape analysis (PSA). This technique is not new, and has been proposed with variable results [5-10]. In recent years DPSA techniques of both current and charge signals, produced by charged particles penetrating solid-state detectors, have been proposed as a PID tool with very promising results [11-15]. In these works various analytical techniques for DPSA have been applied for identifying ions down to 2 MeV with neutron transmutation doped (NTD) silicon detectors. These pulse shape discrimination was based both in simple calculations (signal amplitude, rise time, decay time, rise slope) and more advanced ones (correlation between second and third order moment of the time distribution signals). The combination of the three techniques (TOF, ELOSS, DPSA) should improve the PID efficiency of the new generation of particle detectors being currently built.

The use of Artificial Neural Networks (ANNs) is a very promising alternative to the mentioned DPSA techniques. The use of ANNs has been reported for a number of nuclear physics applications, like trigger function [16], extracting information from heavy ion reactions [17], Bragg curve spectroscopy [18] and some others [19-22]. The ANN particle identification could easily be implemented in an electronic device (i.e. on a FPGA) for on-line analysis, decreasing the amount of data to be stored and simplifying the corresponding off-line analysis. Some chips have already been designed specifically to implement ANNs on dedicated data acquisition systems [23, 24]. The aim of this paper is to contribute to this trend by analyzing the performance of ANNs as a particle identification tool for low energy heavy ions impinging on silicon detectors.

2. Artificial neural networks for DPSA

An artificial neural network consists of a set of artificial neurons, typically organized into several layers with a high degree of interconnection. Among the different existing topologies of neural networks [25], recurrent networks, radial-basis function networks and feed-forward networks have been studied for PID by PSA. The "recurrent networks" have feedback links between some layers, and the "radial-basis function networks" possess different type of neurons. We have found that the recurrent networks presented a lower performance in some initial tests. The networks based on radial-basis function neurons, such as the probabilistic neural network (PNN), don't require an iterative learning algorithm, but need a very high number of neurons. This may become a problem for the software tools that limit the total number of neurons. The Feed-Forward or Multilayer Perceptron (MLP) network shows very good results in many different applications where there is a complex, non-linear relationship between several variables. Therefore, in this paper we have first focused on the application of MLP networks to DPSA.

The MLP topology typically consists of two or three neuron layers and an input layer where the network receives in a parallel way the whole set of the input values. Each layer is fully interconnected with the preceding and subsequent layer. A schematic representation of the MLP topology and the operation of their neurons is shown in Fig. 1. The first layer doesn't contain neurons, but only send the input values to the first hidden neuron layer. For the purpose of this research, the input units contain the sampled values of the digitized pulse shape. The network can be configured with one or two hidden neuron layers, and an output one. In the MLP networks, the artificial neurons work as processing units where a given linear combination of the inputs gives a neuron output through a particular transfer function *f*. These linear combinations have an array W of weights w_i as coefficients and may also contain a constant term, the bias b. The transfer functions of the neurons can be linear or non-linear. For the purpose of solving complex relationships between the input and output variables, at least one layer must use non-linear functions such as "log-sigmoid" or "tan-sigmoid" (see Table 1). In this work the use of different combinations of the transfer functions has been analyzed, showing similar results. Linear transfer functions may also be used for the output layer.

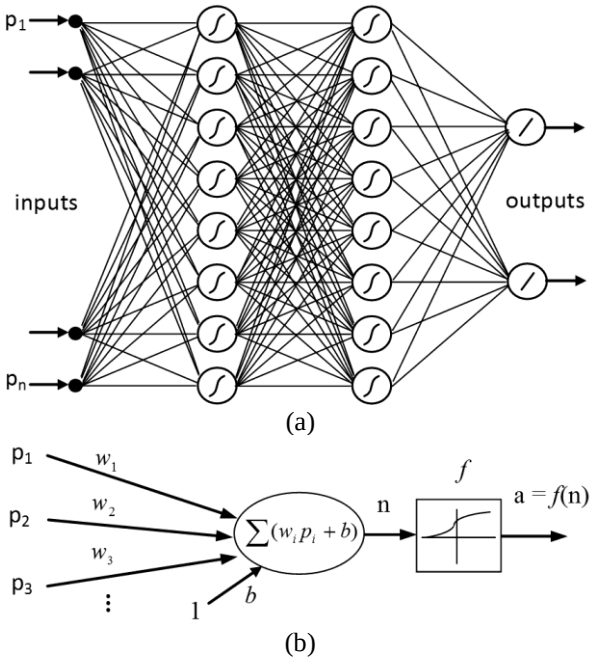

Fig. 1. (a) Schematic representation of the MLP network topology containing *n* input units, two 8-neuron hidden layers and 2 neurons in the output layer. (b) Detail of the neuronal function.

Table 1. Typical transfer functions for neurons in MLP networks.

Linear	Log-Sigmoid	Tan-Sigmoid
$a = n$	$a = \frac{1}{1+e^{-n}}$	$a = \frac{2}{1+e^{-2n}} - 1$

The MLP network belongs to a type of ANN with supervised learning. It uses a given set of input-output learning pairs for the adjustment of the interconnection weights. The iterative "Back-propagation" learning algorithm is applied to adjust the weight array *W* associated with the links. For each learning cycle the input vectors (organized in the *input matrix array, P*) is given to the ANN. Then the output vectors are compared with the result of the learning pairs (organized in the *output matrix array, T*), and the mean square error (*mse*) is calculated. The mathematical method of back-propagation determines the re-adjustment of the weights to reduce the *mse* iteratively until it reaches a satisfactory value. The number of neurons in hidden layers is usually not too high (less than 20 for many applications), and the optimum value is selected after some tests of convergence. Once the array *W* has been obtained with the initial training data set, new input-output pairs not used during the training stage are used as validation data to test the network performance in terms of generalization capability. The Neural Network Toolbox of MatLab© was chosen for the design and training of the ANNs, running in a standard Personal Computer with a Core 2 Duo Processor and 2 GB RAM. Using

100 training pairs for each isotope, with a training goal of mse $=10^{-6}$, the training process takes a time of about 10 minutes. Among the different available back-propagation algorithms, the Levenberg-Marquardt technique was found to be the fastest for achieving the accuracy goal and it was used for all the training cycles.

In this work it is analyzed the performance of DPSA technique making use of digitalized current signals produced by energetic heavy ions (total kinetic energy between 96 and 688 MeV) impinging directly on silicon detectors. The data under study were obtained in experiments performed by the FAZIA collaboration [27] using the CIME cyclotron at the GANIL facility in Caen, France. In these experiments, a high homogeneity Neutron Transmutation Doped (NTD) detector, 300 microns thick, 200 mm2, was bombarded by 20 different isotopes from ^{12}C up to ^{84}Kr. The energy of the beam was between 7.39 and 8.68 MeV/u. The detector was mounted in rear (n-side) injection configuration, which facilitates the identification process [5-7]. The applied voltage was fixed at a value of 190 V (depletion voltage 140 V). It was connected to a 300 MHz bandwidth preamplifier (PACI, developed by the Orsay group of FAZIA [13]), mounted very close to the detector, 4 cm, inside the vacuum chamber, providing analog charge and current outputs. The current signals were recorded using a commercial ACQIRIS data acquisition system (2 GS/s, 8 bits digitizer). All the signals from the different ions were stored using the same amplitude scale. The PACI charge output was sent to a shaping analog electronics to measure the energy with a peak-sensing ADC. In every run of the experiment they used "mixed" beams with known isotopes, all of them with different mass and charge to mass ratio, but same energy per nucleon. Therefore the identity of each pulse was determined by the energy measurement. A more detailed description of the setup and data processing is given in [14].

As a first approach to the problem, we have designed our ANNs to be able to classify the current signals producing pairs of numbers. These pairs of numbers could be arbitrary ones, but we have chosen meaningful numbers related to the pairs (N,Z) (neutrons, protons) of the set of isotopes under investigation. For each isotope of the training data set, a determined output is assigned using proportional numbers to the N and Z values. Thus the ANN contains 2 output neurons. After the iterative training with the input and output matrices, the resulting neural network can be tested to check its performance using a different set of pulses not used during the training stage.

The pulses obtained in our measurements are typically less than 300 ns in length, with a time step of 0.5 ns, producing input vectors of a maximum of 600 components. Although this vector would be a suitable input for our ANNs, we found that good performance could be obtained in some cases with half of the components (time step of 1 ns). In the results presented below either a 0.5 ns or a 1 ns time step was used, so that the highest number of elements of the input vectors, and the number of units of the ANN input layer, is 300. This choice is consistent with the use of the 300 MHz PACI preamplifier. The ANNs used in this study

consist of two hidden layers, with a number of neurons between 5 and 10 in each layer. For the training process we have used, for each isotope, only 100 current signals. However, the tests of performance were carried out with 2000 events to assess the method consistently. In the next section we apply this method to a large group of isotopes with selected values of energy per mass unit as produced by the CIME cyclotron (absolute energies ranging from 117 MeV to 168 MeV). In section 4 the method will be used to classify pairs of isotopes of similar energy.

3 DPSA studies for a "large" set of isotopes

In this section the performance of MLP networks using a wide group of (N,Z) values and energies is studied. Among the available data we have chosen the following isotopes for the ANN training: ^{16}O at E=131 MeV, ^{32}S at E=135 MeV, ^{20}Ne at E=156 MeV and ^{40}Ar at E=168 MeV. Beside the early isotopes, other isotopes will be used as inputs to the trained ANN in order to study their classification, despite of the fact that they are not considered in the training phase. These isotopes are ^{15}N at 117 MeV, ^{28}Si at 117 MeV and ^{36}Ar at 151 MeV. To illustrate the complexity of the experimental scenario, we have plotted in Fig. 2 several current signals produced by the set of ions under study. Despite the differences in energy, there exist large similarities between pairs of isotopes (^{16}O, ^{20}Ne), (^{32}S, ^{40}Ar), (^{28}Si, ^{36}Ar). This is due to a complex interplay between the plasma ionization process and the implantation depth of energetic ions in the NTD silicon wafer, leading to similar charge collection rates. The effect can be better seen in Fig. 3, where the averaged value of 2000 pulses is shown for every isotope. The MLP network has been trained using 100 current pulses of ^{16}O, ^{20}Ne, ^{32}S, ^{40}Ar, with an output corresponding to their N and Z values. No higher performance could be observed by using more training pairs, and a slightly reduced performance could be observed in case of using 50 pulses per isotope or less. Furthermore, the use of different amounts of training pairs for the different particles was not relevant, assumed that they are not very few. Baseline corrections for current pulses were introduced as given in [14].

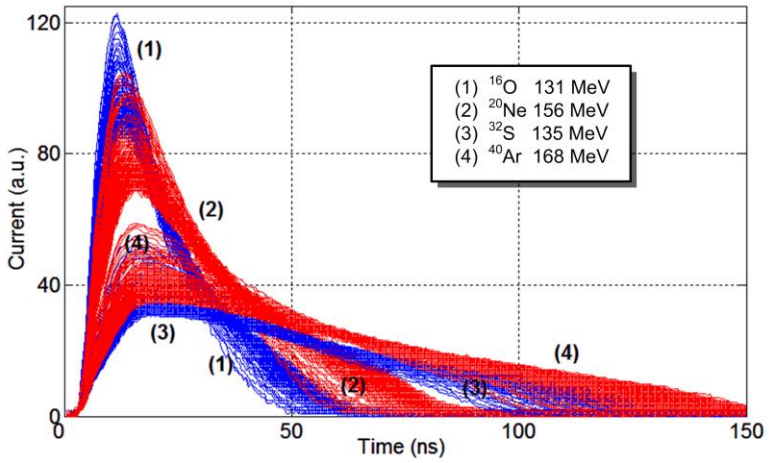

(a)

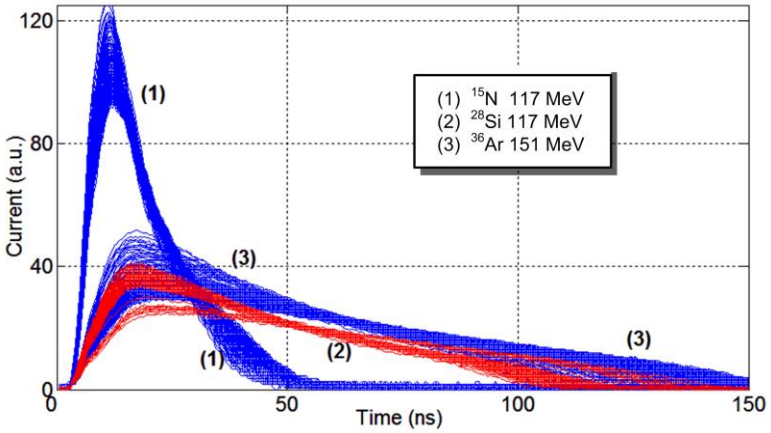

(b)

Fig. 2. (a) Current pulses of ^{16}O, ^{20}Ne, ^{32}S, ^{40}Ar used at ANN training stage. (b) Current pulses of ^{15}N, ^{28}Si and ^{36}Ar, not included in training stage; they were used to test ANN generalization capabilities.

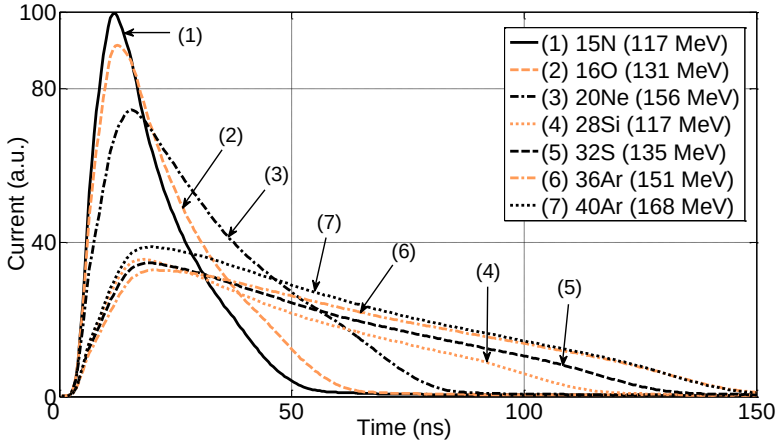

Fig. 3. Averaged pulse shapes of the 7 different isotopes of Fig. 2.

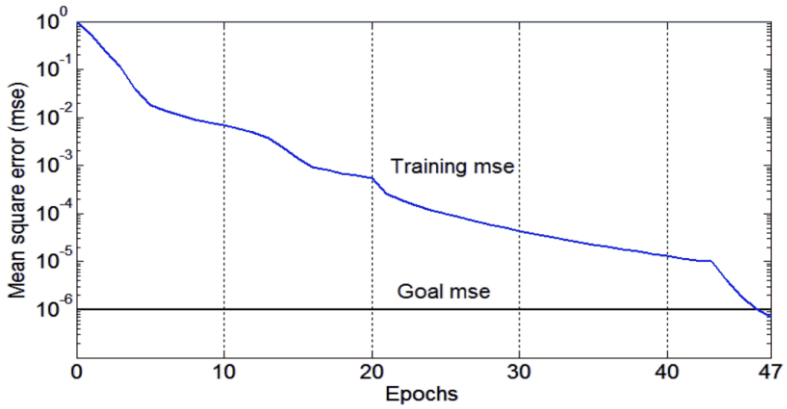

Fig. 4. Progress in the learning process achieved along the training stage. In the figure the *mse* value is plotted as a function of the corresponding *epoch* (learning cycle). The goal was stablished at *mse* = 10^{-6}.

The ANN used in this work had the input layer and three neuron layers with a N-8-8-2 structure, being N the number of samples and containing a total of 18 neurons (see Fig. 1). We have used 300 samples per current pulse (time step of 0.5 ns), and the corresponding Levenberg-Marquardt back-propagation algorithm. Tan-sigmoid transfer functions were chosen for hidden layers and a simple linear function for the output. Neural networks typically achieve better performance with input and output values around the unity. Therefore a scale factor of 1/70 was applied to the input pulses, and a scale factor of 1/16 for the (N,Z) goals, to give ANN input and output values under 1.5. With this configuration a training goal of *mse* =10^{-6} was achieved in 46 iterations (epochs), corresponding to about ten minutes of computing in our PC. Fig. 4 shows the training error convergence versus number of iterations (epochs). After the training stage using 100 pulses per isotope, the resulting ANN was validated with 2000 events of each isotope. The results have been plotted in Fig. 5 using a 2-dimensional diagram, representing the N value in the x-axis and the Z value in the y-axis. It can be noted various clusters of points centered on the corresponding (N,Z) pairs. In the case of events of the 4 isotopes used for the training, the distance between a given (N,Z) pair and the actual value is inversely related to the degree of "likelihood" between the input signal and any of the training patterns. A clear separation between isotopes was obtained in the validation stage showing a large identification success (≈ 100%). To study the generalization capabilities of our ANN, we have tested the system with a set of isotopes not included in the training stage, and therefore completely "unknown" by the ANN. This is equivalent to the case of a nuclear reaction producing exotic fragments for which the system had not been previously trained and calibrated. We may not expect to obtain the correct N and Z values for such unknown isotopes, but only to get different outputs, clearly separated from the other. For this purpose we have chosen from our database the set of isotopes: ^{15}N at 117 MeV, ^{28}Si at 117 MeV and ^{36}Ar at 151 MeV. The results are also plotted in Fig. 5. In this case we also observe clusters located

in some particular regions, well separated from the other clusters, and thus providing a tool to classify nuclear species not included in the original training process.

In order to quantify the "classification capability" of our ANN, the degree of overlap between neighbouring clusters can be measured. For this purpose it is often used the so-called *factor of merit* M introduced in [26] for gamma-neutron discrimination, which was also applied to DPSA in [14]. Here a 2-dimensional generalization is introduced as:

$$M = \frac{\left\|\vec{\mu}_1 - \vec{\mu}_2\right\|}{(\sigma_1 + \sigma_2)\cdot 2.35} \tag{1}$$

where μ_i ,σ_i (i=1,2) are the corresponding 2-dimensional centers and standard deviations of the clusters respectively,

$$\vec{\mu} = \frac{\sum_{i=1}^{n}(N_i, Z_i)}{n} \tag{2}$$

$$\sigma = \sqrt{\frac{\sum_{i=1}^{n}\left\|(N_i, Z_i) - \vec{\mu}\right\|^2}{n-1}} \tag{3}$$

Using this prescription, values of the factor of merit M > 0.75 can be associated to a good rejection rate, and when M > 1 almost all the events are fully separated. For the "unknown" set the corresponding factors of merit yielded the following values: M(^{15}N-^{16}O) = 1.74, M(^{28}Si-^{32}S) = 0.90 and M(^{36}Ar-^{40}Ar) = 1.73. These values show a good rejection rate in the worst cases, that is, the isotopes whose clusters are nearest. So, ANNs can be used as a good classifier. Due to the limited number of isotopes available for the training stage, we could not expect the ANN to assign the exact (N,Z) values, but as we can see they were classified in well separated clusters and in regions not far away from the actual values. For future studies it would be desirable to introduce an energy filter at the first stage, and also a larger set of isotopes to provide enough (N,Z) data for the training process. Besides, higher accuracy could be obtained by increasing the complexity of the ANN in terms of neurons and layers, training with higher amounts of events and running the learning process during more epochs.

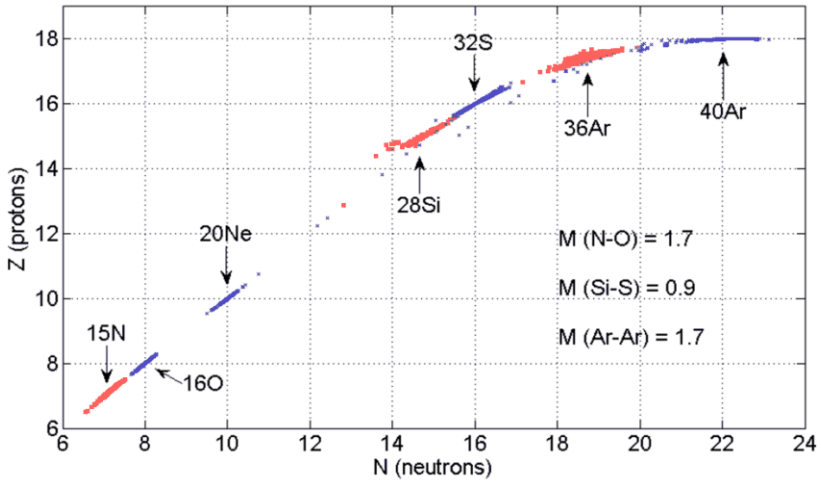

Fig. 5. ANN output for 2000 events per isotope. ANN trained with ^{16}O, ^{20}Ne, ^{32}S and ^{40}Ar. Including in test the unknown isotopes ^{15}N, ^{28}Si and ^{36}Ar.

4. Discrimination between pairs of isotopes at similar energy

In this section the discrimination capabilities of the ANNs in the less favourable cases, that is, pairs of isotopes of the same element and at similar energy, are analysed. This type of analysis has been carried out [14] using analytical parameters like rise time, decay time, signal amplitude, slope and 2nd and 3rd order moment of the shapes, because of the difficulty of a more direct analysis of so similar pulse shapes. For this study we have chosen the pairs of isotopes ^{12,13}C, ^{36,40}Ar, ^{80,84}Kr, that are analysed independently. The isotopes were accelerated at the CIME cyclotron with similar energy (see Table 2). Different energies ranges have been considered in this analysis, from 96 MeV Carbon isotopes to 677 MeV Krypton isotopes.

Table 2. Mean total energy of the events saved from the experiment for the 3 pairs of isotopes used for this analysis.

Isotope	Mean total energy	Isotope	Mean total energy
^{12}C	98.48 MeV	^{13}C	96.74 MeV
^{36}Ar	313.10 MeV	^{40}Ar	313.00 MeV
^{80}Kr	688.40 MeV	^{84}Kr	677.00 MeV

The best configuration of the neural network has been the same ANN topology and size used previously, that is N-8-8-2. In this case, the time step has been increased to 1 ns without any loss in the classification capacity (as we can see later). The training process has the same characteristics than in the early case, that is, 100 pulses for learning process and 1000 pulses for validating process of each isotope. For the same reason that in section 3, some scale

factors were applied to the values of the pulses and the goals to facilitate the ANN working with values around the unity.

The experimental data for the case of ^{12,13}C isotopes is shown in Fig. 6, considering only the first 50 samples per pulse, time step of 1 ns. However, the input vectors used contained 100 elements (100 ns time and 100 ANN inputs). The shape of the pulses are very similar for both isotopes, but some difference can be found in the average shapes (1000 samples) which will help the ANN to classify the data in a pulse-by-pulse basis. The classification results obtained are shown in Fig. 7. It shows a remarkable success rate of 98.3% (983 out of the 1000 pulses have been well classified for each isotope), considering as correct the N values in interval (5.5,6.5) for ^{12}C and interval (6.5,7.5) for ^{13}C. The factor of merit M was 1.71. Therefore, an ANN with a correct training can use the minimum difference in similar size and energy to obtain a correct classification.

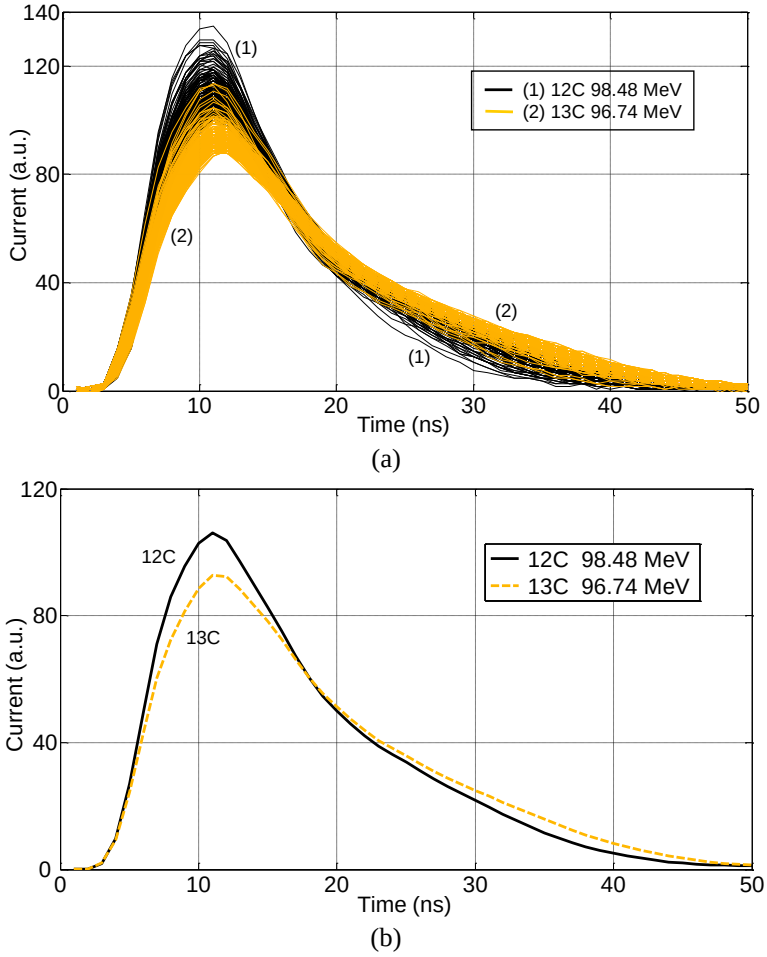

Fig. 6. Data set for the pairs of isotopes (^{12,13}C) showing the first 50 samples of the 100-element ANN inputs. (a) Individual pulse shapes. (b) The average of 1000 pulses.

The "success rate" or efficiency of the ANN for the task of discrimination between pairs of similar isotopes has been evaluated considering the success as the output value inside a unity interval around integer values of N. If a more narrow interval is considered for the "success counts", the efficiency decreases a bit, but the "purity" is increased, with a lower number of misidentifications.

The method was also applied to Argon and Krypton isotopes using input vectors of 200 and 300 elements, respectively. This is due to the larger duration of the current pulses with increasing ion mass, almost 200 ns for Argon and 300 ns for Krypton. The results are shown in Fig. 8, with factors of merit M = 0.76 and M = 0.98 for Ar and Kr isotopes respectively, also showing an acceptable rejection rate. The conclusions obtained in the study of ^{12,13}C isotopes are maintained in the studies of Argon and Krypton isotopes.

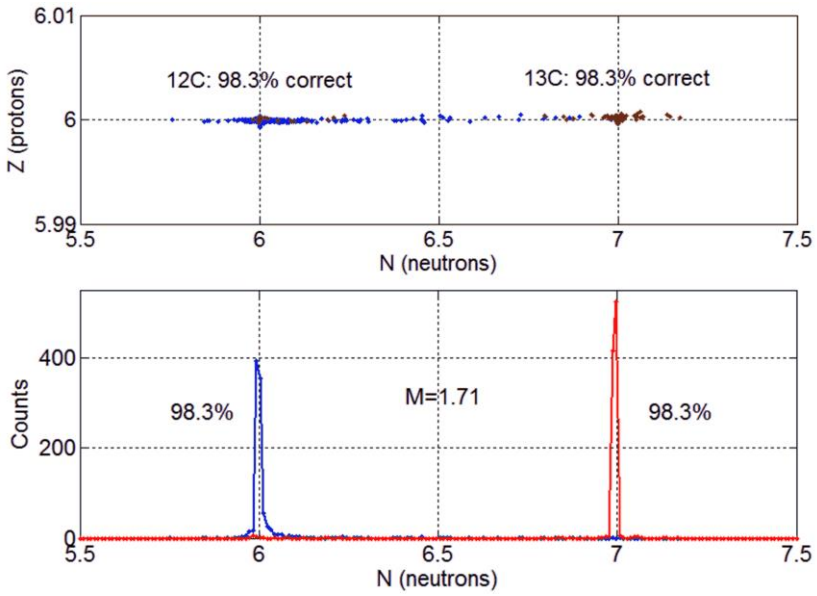

Fig. 7. N-Z discrimination of ^{12,13}C isotopes. N-Z plot with the output space of the ANN for 1000 pulses (top). Projection over the N axis (bottom). Separation cut on N=6.5.

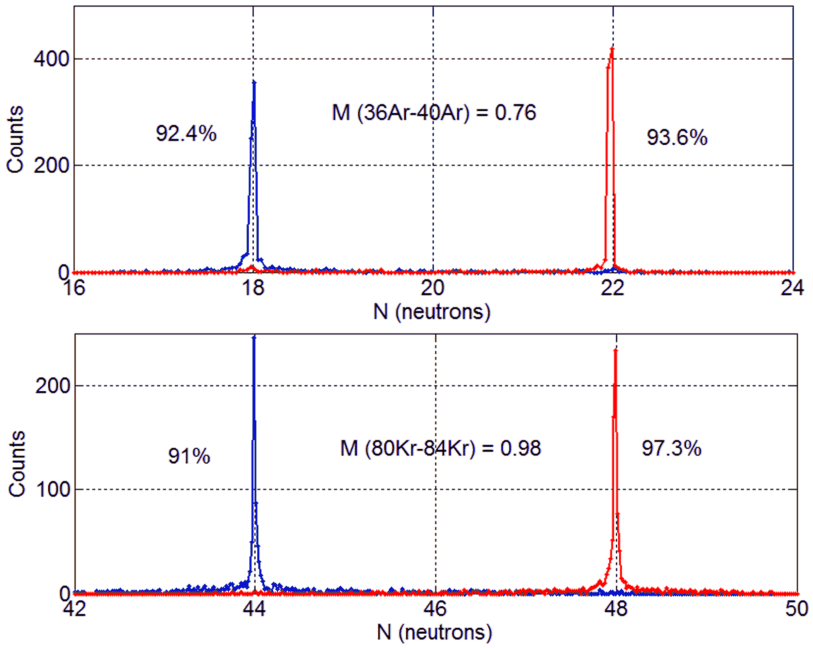

Fig. 8. Discrimination (projection over the N axis) of ^{36,40}Ar (top) and ^{80,84}Kr (bottom). Separation cut on N=20 and N=46, respectively.

5. The method of differential shapes

In previous sections we have used the raw data as the input of our ANN, and reasonable discrimination capabilities with M > 0.75 has been found. In this section we investigate a second method, with a pre-processing of the input pulses, in order to improve the success rate. This method is based on subtracting from each event the mean pulse shape of all the events under analysis, and then using the resulting signals as the input for the ANN. In this way the structural components common to the pulse shapes are removed, remaining only the specific features and thus enhancing the differences. For now on we will refer to this method as the "differential shape" method, leaving the term "standard" for the previous one. For the sake of simplicity, we have applied this recipe only to the pairs of isotopes studied in last section. To illustrate the new analysis scenario, in Fig. 9 we show the pulse shapes resulting from average pulse subtraction for the case of Krypton isotopes, which will be the inputs for the ANN. It should be noticed the large duration of the current signals for these medium mass ions, which extend as long as 300 ns. On the other hand, large deviations from the average shape are found at the beginning and at the end of individual pulses, suggesting the need to store the complete pulse shape to perform detailed particle identification.

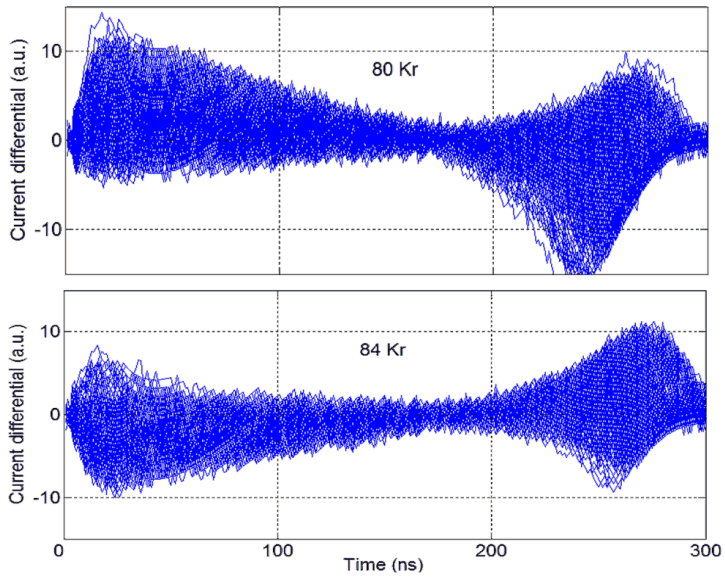

Fig. 9. Pulses of ^{80}Kr (top) and ^{84}Kr (bottom) isotopes after average pulse shape subtraction. The average pulse is subtracted from the individual pulse shapes.

The first consequence of the "differential shape" method is a shorter training process, achieving the mse goal in only a few epochs. The second consequence is an improvement in the ANN performance, as can be observed in Fig. 10. A comparison between both methods is shown in Table 3. In all isotopes, the factor of merit *M* shows a significant improvement. It is remarkable that the differential shape method provides higher discrimination rates than the former ones and the one proposed in [14] using analytical techniques.

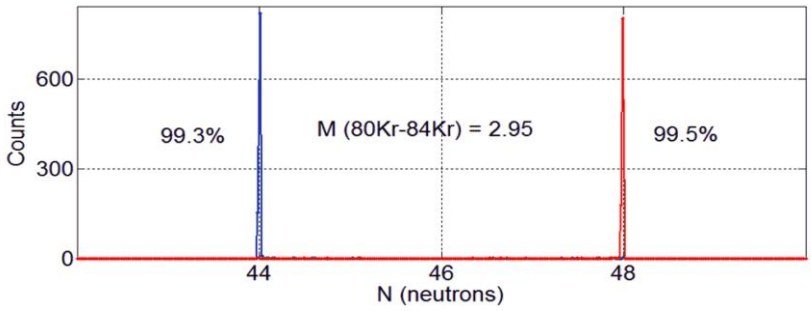

Fig. 10. Discrimination (projection over the N axis) of ^{80,84}Kr isotopes with the method of differential shapes.

Table. 3. Identification success and figures of merit obtained by the "standard" method and the one using "differential" methods.

	Standard		Differential	
Isotope	Success (%)	M	Success (%)	M
^{12}C - ^{13}C	98.3 - 98.3	1.71	100 - 99.4	4.48
^{36}Ar - ^{40}Ar	92.4 - 93.6	0.76	98.1 - 90.2	0.90
^{80}Kr - ^{84}Kr	91 - 97.3	0.98	99.3 - 99.5	2.95

6. Conclusions

The use of Artificial Neural Networks for particle identification with silicon detectors based on Digital Pulse Shape Analysis has been evaluated. A Multilayer Perceptron neural network has been chosen, with three neuron layers and N-8-8-2 structure, with N samples per pulse and a total of 18 neurons. The MLP network has been trained and validated using current pulses with a sampling rate of 1 ns, each pulse containing between 100 and 300 samples.

The verification of the neural network as an identification method has been performed with heavy ion data obtained from previous experiments carried out with the CIME cyclotron at GANIL (Caen, France) in a range of energies between 4-9 MeV/u using NTD silicon detectors, corresponding to a total energy between 96 and 688 MeV.

First the ANN has been applied to classify ^{16}O, ^{20}Ne, ^{32}S and ^{40}Ar ions imposing an output value corresponding to their N and Z values. The results confirm that the method is able to assign neutron and proton number successfully. The ANN performance has also been tested using isotopes not used during the training stage, which could occur in a generic nuclear reaction. The results for ^{15}N, ^{28}Si and ^{36}Ar isotopes, which were not included in the training stage, have been presented and discussed. In this study, all isotopes (included or not in the training process) are clustered and differentiated, obtaining a factor of merit M above 0.9 for the nearest clusters of outputs. Therefore, the neural network can be used as a good classifier of particles.

The ANN classifier has been also tested in the worst situations, that is, classifying isotopes with similar size and energy. The cases of $^{12,13}C$, $^{36,40}Ar$, $^{80,84}Kr$ have been considered. In these cases, a direct pulse shape analysis achieves a discrimination rate above 91%. It is not very high due to the similarity among the pulse shapes.

A new method of ANN analysis, referred as "differential shape method", is presented and investigated. This new method has the objective of improving the performance of the ANN training process and the success rate when discriminating between a pair of similar ions. It consists of using the difference between a certain shape and the mean shape of both ions in order to classify the particles. In this case we obtain a discrimination rate above 98%, higher than any other previously reported work.

In summary, an artificial neural network, and more exactly a multi-layer perceptron, is a good classifier of particles impinging on silicon detectors. The kind of measurements used to evaluate the results have shown a success rate (the rate of a correct identification), above 90% in all cases, and a factor of merit M above 0.9 in all cases. Besides, this method can be used to discriminate isotopes of similar sizes and energies, cases in which a direct pulse shape analysis is difficult. Finally, a new method including a pre-processing prior to the execution of the ANN has been studied. This method, consisting in processing the difference between a certain pulse and the mean pulse of the pair of similar isotopes, has shown to include improvements in the training time and in the factor of merit M with respect to the cases without the pre-processing stage.

Acknowledgments

The authors are grateful to the FAZIA collaboration [27] for providing part of the experimental data used in the present study. This work has been supported by the Spanish Ministerio de Economía y Competitividad under the grant FPA2014-59954-C3-1-P, by the Andalusian Conserjería de Innovación, Ciencia y Empresa, under the grants FQM 4964 and P10-TIC-6311, and by the European Union Seventh Framework Programme FP/2007-2013 under Grant Agreement n. 262010-EN-SAR.

References

[1] GANIL, Grand Accelerateur National d'Ion Lourds, Caen, France. SPIRAL2 Project, Second Generation System On-Line Production of Radioactive Ions.

[2] FAIR, Facility for Antiproton and Ion Research, GSI, Darmstadt, Germany.

[3] LNL, "Laboratori Nazionali di Legnaro", www.lnl.infn.it.

[4] EURISOL, "European Isotope Separation On-Line Radioactive Ion Beam Facility", www.eurisol.org.

[5] C.A.J. Ammerlaan, et al., "Particle identification by pulse shape discrimination in the p-i-n type semiconductor detector" Nucl. Instr. and Meth. 22 (1963) 189.

[6] G. Pausch et al., "Particle identification in solid-state detectors by means of pulse-shape analysis - results of computer simulations", Nucl. Instr. and Meth. A 337 (1994) 573.

[7] G. Pausch et al., "Identification of light charged particles and heavy ions in silicon detectors by means of pulse-shape discrimination", IEEE Trans. Nucl. Science, vol.43, no.3, June 1996.

[8] G. Pausch et al., "Limitations of the pulse shape technique for particle discrimination in planar Si detectors", IEEE Trans. Nucl. Science, vol.44, no.3, June 1997.

[9] P. Guazzoni, et al., “Particle identification via pulse shape analysis for large-area silicon detectors of the CHIMERA array”, IEEE Trans. Nucl. Science, vol.52, no.5, October 2005.

[10] M. Agostini, GERDA Collaboration, et al., “Results on neutrinoless double beta decay of 76Ge from GERDA Phase I” Journal of Physics G: Nucl. Part. Phys., 40 (2013), p. 035110.

[11] L. Bardelli, et al., “Application of digital sampling techniques to particle identification in scintillation detectors”, Nucl. Instr. and Meth. A 491 (2002) 244.

[12] L. Bardelli et al., “Time measurements by means of digital sampling techniques: a study case of 100 ps FWHM time resolution with 100 MSample/s, 12 bit digitizer”, Nucl. Instr. and Meth. A 521 (2004) 480-492.

[13] H. Hamrita et al, “Charge and current-sensitive preamplifiers for pulse shape discrimination techniques with silicon detectors”, Nucl. Instr. and Meth. A531 (2004) 607.

[14] S. Barlini et al, “New digital techniques applied to A and Z identification using pulse shape discrimination of silicon detector current signals”, Nucl. Instr. and Meth. A 600 (2009) 644-650.

[15] S. Kupny, et al., “Charged-particle flow measured with the KRATTA detector in the ASY-EOS experiment”, EPJ Web of conferences 88, 01010, April 2015.

[16] H. Kolanoski, “Application of artificial neural networks in particle physics”, Nucl. Instr. and Meth. A 367 (1995) 14-20.

[17] S. Aiello, et al, “A neural approach to the analysis of CHIMERA experimental data”, Proceedings of Computing in High Energy and Nuclear Physics - CHEP2000, Padova, Italy, 7-11 February 2000, p. 41.

[18] J.J. Vega, R. Reynoso, “Application of neural networks to pulse shape analysis of Bragg curves” Nucl. Instr. and Meth. B 243 (2006) 232-240.

[19] U. Müller, “Artificial intelligence – applications in high energy and nuclear physics”, Nucl. Instr. and Meth. A 502 (2003) 811-814.

[20] S. Athanassopoulos et al, “Nuclear mass systematics using neural networks”, Nuclear Physics A 743, no. 4 (2004) 222-235.

[21] Zhang Caixun, et al., “Discrimination of neutrons and γ-rays in liquid scintillator based on Elman neural network”, arXiv 1509.06259 (Sept 2015).

[22] T. Tambouratzis, D Chernikova, I. Pazsit, “A comparison of artificial neural network performance: the case of neutron/gamma pulse shape discrimination”, IEEE Symposium on Computational Intelligence for Security and Defense Applications (CISDA), April 2013, pp. 88-95.

[23] W. Eppler, T. Fischer, H. Gemmeke, T. Köder, R. Stotzka, “Neural Chip SAND/1 for Real Time Pattern Recognition”. IEEE Transactions on Nuclear Science, Vol. 45, No. 4, pp. 1819-1823. (1998).

[24] R. Jiménez et al, “Implementation of a neural network for digital pulse shape analysis on a FPGA for online identification of heavy ions”. Nucl. Instr. And Meth. A 674 (2012) 99-104.

[25] S. Haykin, “Lessons on adaptative systems for signal processing, communications and control”, IEEE Signal Processing Magazine, pp 39-48, Sept. 1999.

[26] R.A. Winyard, J.E. Lutkin, G.W. McBeth, “Pulse shape discrimination in inorganic and organic scintillators”, Nucl. Instr. and Meth. 95 (1971) 141.

[27] FAZIA, “Four pi A and Z Identification Array”, Project for a new 4-pi array with charge and mass identification using digital electronics signal processing and designed for isospin studies in nuclear physics.